LA-UR-18-24767
Approved for public release; distribution is unlimited.

Title:	Fast Neutron Passive Collar Optimization Report
Author(s):	Root, Margaret A. Geist, William H. Menlove, Howard Olsen
Intended for:	Report
Issued:	2018-06-01

Fast Neutron Passive Collar Optimization Report

FY'18 Optimization of the Fast Neutron Passive Collar for the Verification of LWR Fuel Assemblies

Margaret Root, William Geist, and Howard Menlove

May 2018

1. Introduction: UNCL-II Design

The UNCL has been used for over thirty years for the verification of the ^{235}U content of LWR nuclear fuel. The most recent version of the detector, the UNCL-II, consists of four HDPE blocks, three containing ^{3}He proportional counters and a fourth containing a slot for an AmLi source.[1] The ^{3}He proportional counters have a nominal active length of 33 cm, a diameter of 2.54 cm and a gas pressure of 4 atm. The UNCL-II has cavity dimensions 41.4 x 23.4 x 23.4 cm. A cross-sectional diagram of the UNCL-II enclosing a fuel assembly is shown in Figure 1.

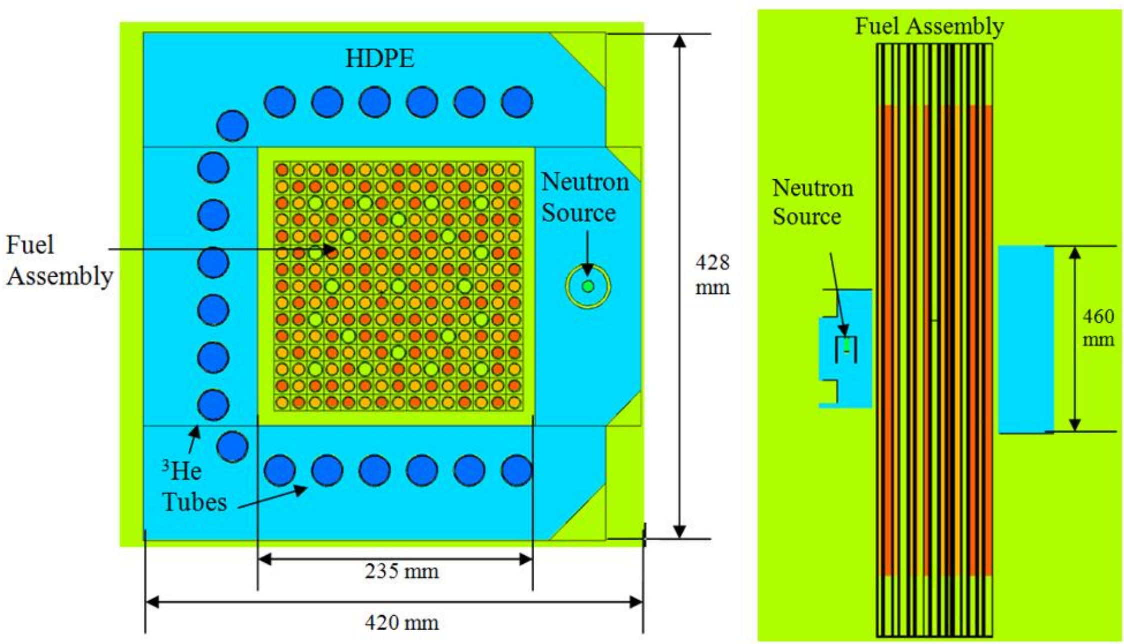

Figure 1: Cross-sectional diagram of the UNCL-II [2].

The Fast Neutron Passive Collar (FNPC) is new, simplified version of the UNCL, which has been optimized using MCNP 6.1 [3] for passive measurements. The new designs are designed to be less sensitive to burnable poisons than previous UNCL designs.

The FNPC uses spontaneous fission neutrons emitted from the ^{238}U in the fuel to induce fission in the ^{235}U, meaning that it operates passively, without an AmLi interrogation source. Two versions of the FNPC are being considered, a ^{3}He-based design and a ^{10}B-based design.

2. Optimization Approach

The optimization of the FNPC considered several factors including the maximizing detector response, minimizing bias caused by burnable poison, minimizing cost, and maximizing usability by IAEA inspectors. The ideal detector system would be one that maximizes the detection efficiency which is in opposition to reducing the cost. Increasing detection efficiency usually corresponds to an increase in cost and increase in size which makes a system more difficult to use. The overall size of the system was constrained to be of similar or smaller size than the current UNCL-II system used regularly by the IAEA. This was chosen as the IAEA has extensive experience in using the UNCL and the size and weight of this system are manageable for use by the inspectors and accepted by the facilities. This would enable the FNPC to be easily assimilated into the IAEA's NDA measurement tools.

The optimization of the ^{3}He and boron based FNPC designs both followed the same general principles. Both systems considered a foot print that was roughly the same size as the UNCL-II system. The length of the systems was increased to maximize the detector response. In an active system, increasing the length of the detector has minimal effect on the response because the the AmLi neutrons only induce fission nearby the interrogation source. For a passive system the interrogation neutrons are evenly distributed through the fuel assembly. Both designs considered liner properties (thickness and material type) and placement location of the detection medium within the polyethylene.

The optimization was based on 7 fuel assemblies used in the Rodeo exercises conducted in 2017 [4]. Four of the assemblies were used to create a calibration curve and three have burnable poison which was used to evaluate the impact of burnable poisons on the design. Details of the fuel assemblies used in the optimization of the designs are given in Table 1.

Table 1: Details of the assemblies used for optimizing the detector design

Type	U-235 Loading (g/cm)	Assembly Description
DU	2.56	204 LEU pins E = DU
LEU	24.46	204 LEU pins E = 2.00%
LEU	37.41	204 LEU pins E = 3.06%
LEU	60.44	204 LEU pins E = 4.95%
BP	25.83	184 LEU pins E = 2.00% 20 Gd pins PWR rod 3.23% w/ 5% Gd
BP	37.51	184 LEU pins E = 3.06% 20 Gd pins PWR rod 3.23% w/ 5% Gd
BP	58.29	184 LEU pins E = 4.95% 20 Gd pins PWR rod 3.23% w/ 5% Gd

^{3}He-based FNPC Design

The ^{3}He and the ^{10}B designs both have detectors on four sides, rather than three sides as in the original UNCL design, as an interrogation source is no longer required. This increases the sensitivity of the detectors to fission neutrons. The MCNP6 [3] model of the basic design of the ^{3}He-based FNPC is shown in Figure 2.

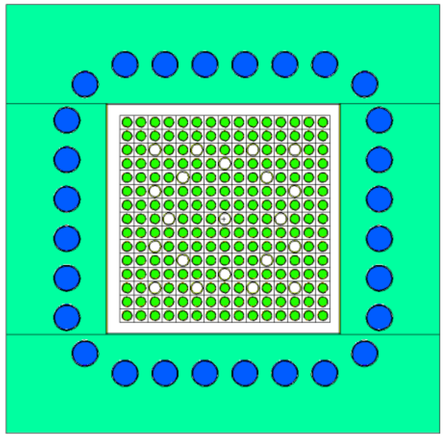

Figure 2: Base design of the ^{3}He-based FNPC, with detector tubes on all four sides of the detector.

a. Tube Length

To optimize the UNCL for passive measurements, the tube length was increased from 33 cm to 43 cm to increase the counting efficiency of the detector, while maintaining a reasonable detector weight for inspection purposes.

b. Pressure

To increase counting efficiency, the pressure used for the proportional counters was increased from the standard 4 atm pressure. The detector efficiency does not increase linearly with increasing pressure, rather the percent improvement in counting efficiency per atm increase in tube pressure begins to decrease at higher pressures as shown in Figure 3. We decided to use a pressure of 6 atm going forward, as it provided the highest efficiency with lower transportation risk and cost than higher pressure tubes.

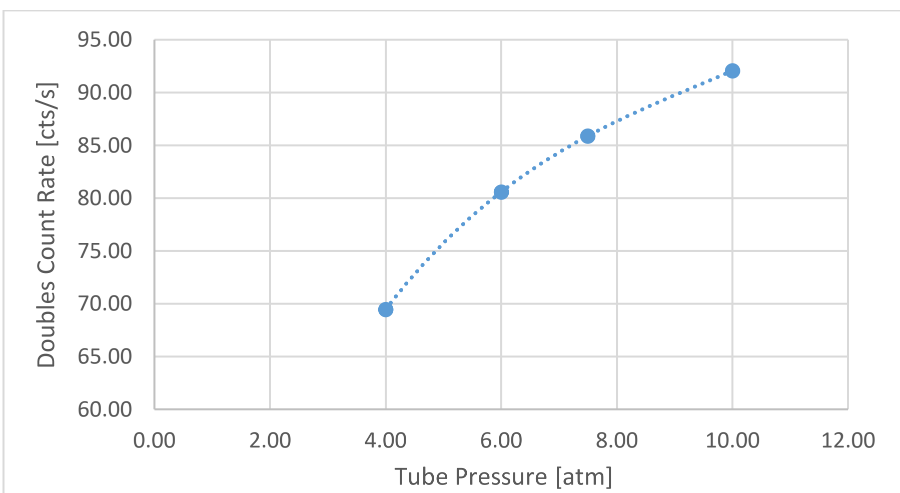

Figure 3: Plot of Doubles count rate (cts/s) vs. tube pressure (atm) for a LWR fuel assembly with a linear density of 60.44 g ^{235}U/cm.

c. Liners

The FNPC requires Cd or Gd liners to prevent thermal neutrons from inducing fissions. The liners were optimized to provide the highest possible count rate, while having the greatest reduction in burnable poison effect. The liner thickness was chosen based on MCNP6 [3] simulations from FY17.

It is important to note that the detector design used in these simulations was significantly different from the design we decided to proceed with for the more recent simulations. The liner simulations were done using two rows of ^{3}He-tubes at 4 atm rather than one row of tubes at 6 atm, as in the current model. This provided higher efficiency, but at much greater cost than the single row of ^{3}He tubes. A rendering of the MCNP6 [3] model is shown in Figure 4.

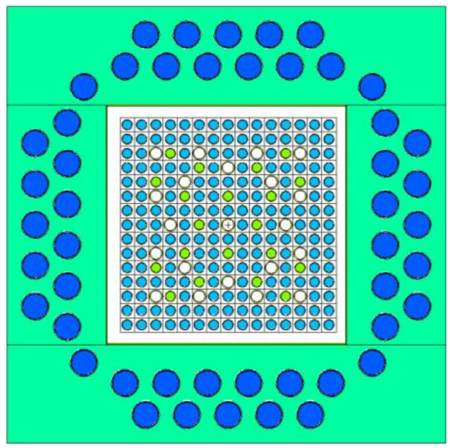

Figure 4: MCNP6 [3] rendering of the two-row version of the ^{3}He-based FNPC.

We simulated the effects of different types and thicknesses of liners, and found that the 1 mm Gd liner provided the least burnable poison perturbation, as shown in Figure 5 and Figure 6. Therefore, the rest of the modeling was done with a 1 mm Gd liner.

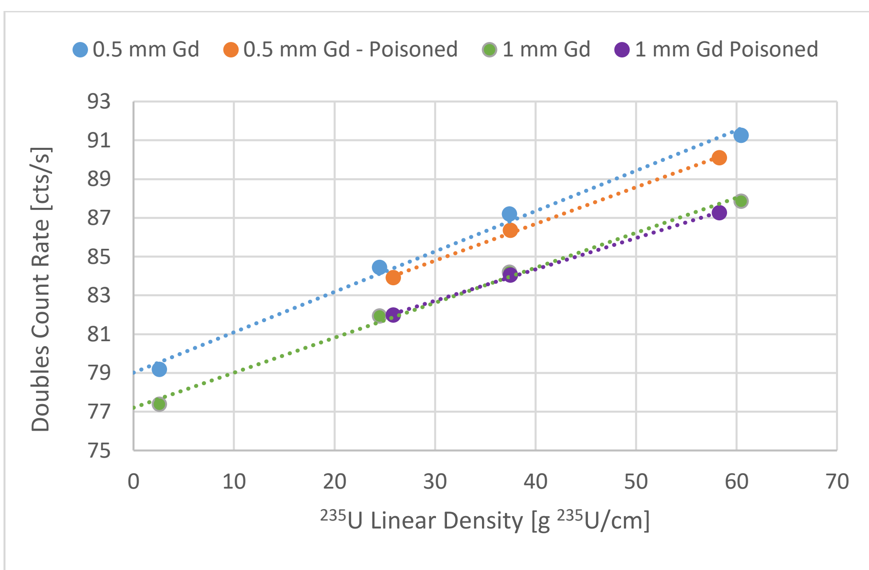

Figure 5: Doubles count rates with 0.5 mm Gd liner and 1 mm Gd liner.

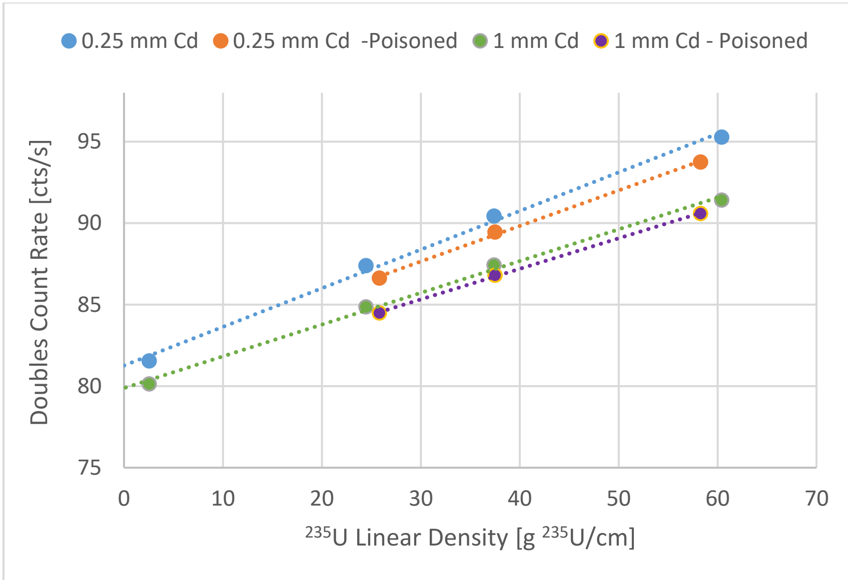

Figure 6: Doubles count rates with 0.25 mm Cd liner and 1 mm Cd liner.

d. Tube Depth

The ^{3}He tube depth was optimized to provide the highest possible doubles count rate. The original design placed the tubes in the center of the polyethylene block, in part to shield the detector tubes from accidental counts. Because accidentals are not a concern with the FNPC, we were able to move the detector tubes closer, to 1.555 cm closer to the fuel assembly than the center of the polyethylene block. As shown in Figure 7, this tube depth provides the highest doubles count rate for a LWR fuel assembly with a linear density of 60.44 g ^{235}U/cm.

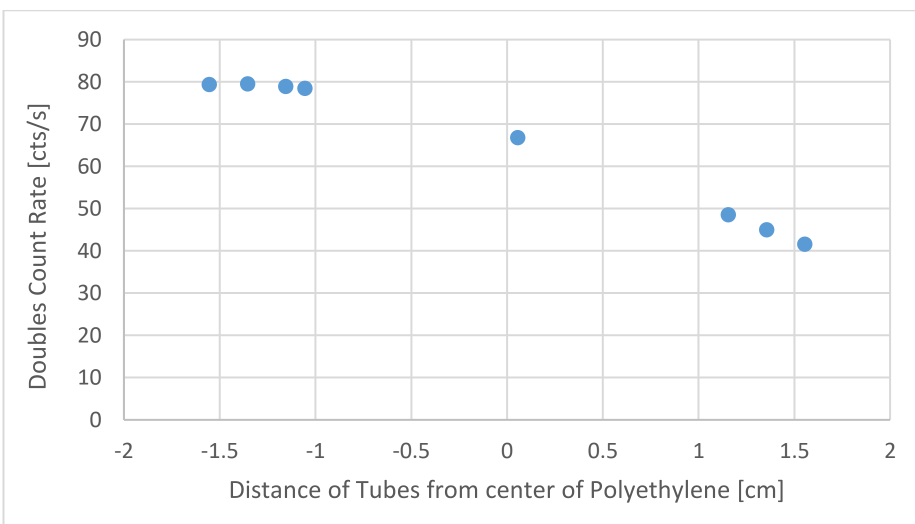

Figure 7: Plot of Doubles count rate (cts/s) vs. distance of detector tubes from the center of the polyethylene block (cm) for a LWR fuel assembly with a linear density of 60.44 g ^{235}U/cm. Negative tube depths are closer to the assembly and positive tube depths are farther from the assembly than the centerline of the polyethylene.

e. Corners

To reduce the detector weight, the corners of the detector were removed. The width of the triangular corner cutout was optimized to provide the greatest weight reduction with the least effect on measured count rates. The optimal corner cutout width was decided to be 5 cm, as it provides the greatest reduction in detector weight for the lowest decrease in doubles count rate as shown in Figure 8. Again, these simulations apply to a LWR fuel assembly with a linear density of 60.44 g ^{235}U/cm.

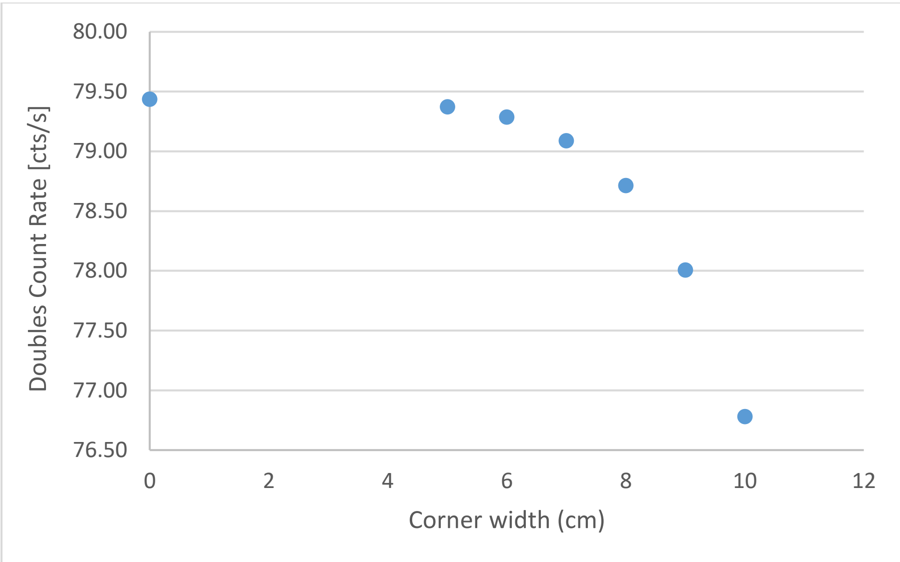

Figure 8: Plot of Doubles count rate (cts/s) vs. corner width (cm) for a LWR fuel assembly with a linear density of 60.44 g ^{235}U/cm.

f. VVER

Triangular cutouts were added to the design to allow VVER fuel to fit within the detector. The cutouts decreased the efficiency of the design, and their inclusion meant that the two center tubes on the two long sides of the detector needed to be moved back and the tubes immediately to the sides of the center tubes needed to be moved forward for the highest possible doubles count rates. A polyethylene insert is also included in the design, which is for use whenever the detector is not measuring VVER fuel. The depth of the tubes was optimized for the case in which the polyethylene inserts are not present, to ensure that the detector would have optimal performance with VVER fuel, as shown in Figure 9, below.

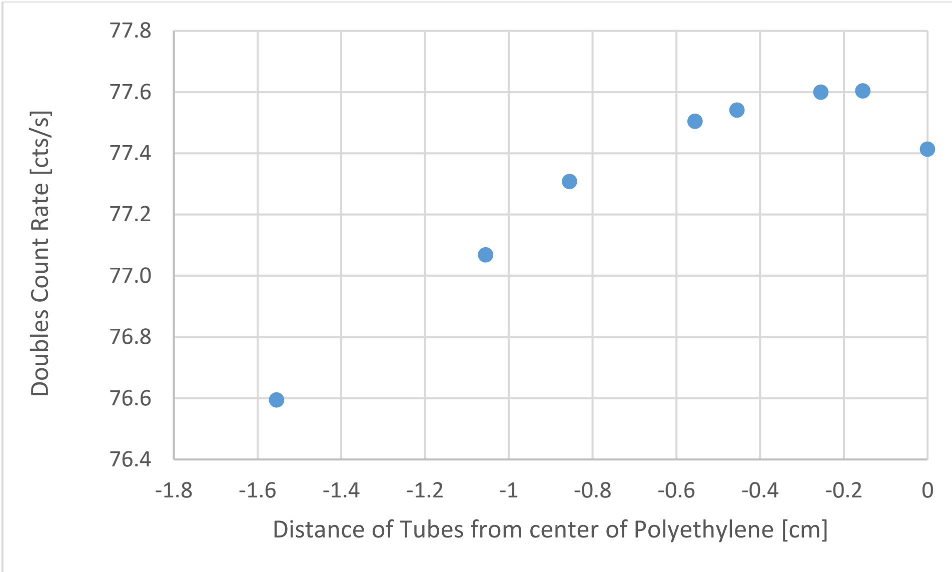

Figure 9: Plot of Doubles count rate (cts/s) vs. the distance of the two inner tubes on the long sides of the detector from the center of the polyethylene slabs (cm) with no polyethylene insert for a LWR fuel assembly with a linear density of 60.44 g ^{235}U/cm.

The optimized distance of the two center tubes from the center of the polyethylene would seem to be somewhere between -0.4 cm and -0.1 cm. As the detector will also need to be used to verify non-VVER fuel, the optimal tube depth in this range with a polyethylene insert included was chosen, which was shown to be -0.355 cm as shown in Figure 10, below.

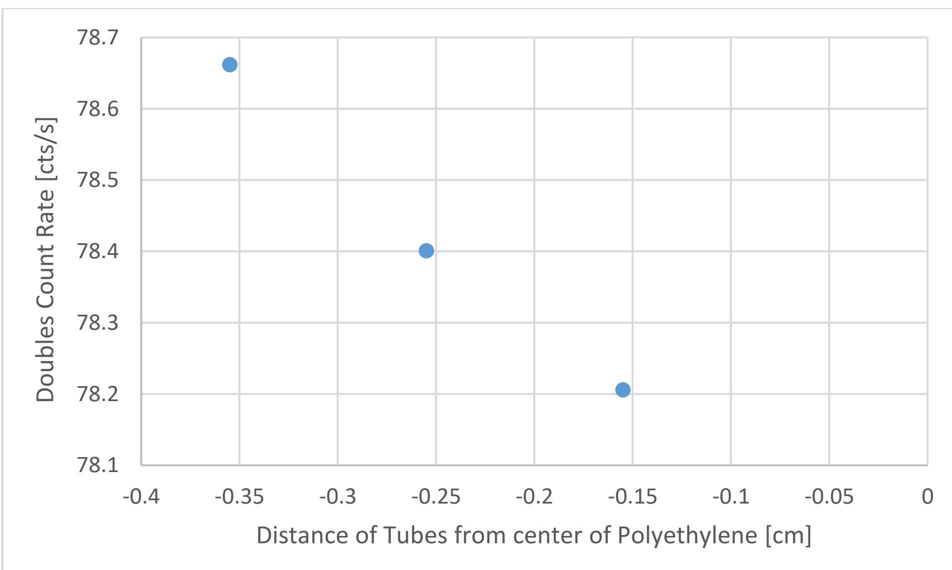

Figure 10: Plot of Doubles count rate (cts/s) vs. the distance of the two inner tubes on the long sides of the detector from the center of the polyethylene slabs (cm) with a polyethylene insert for a LWR fuel assembly with a linear density of 60.44 g ^{235}U/cm.

Finally, the two tubes on either side of the central tubes on the long sides of the detector needed to be moved slightly closer to the assembly than the rest of the tubes, to a position of -1.855 cm from the center of the polyethylene block for the highest possible doubles count rate as shown in Figure 11, below.

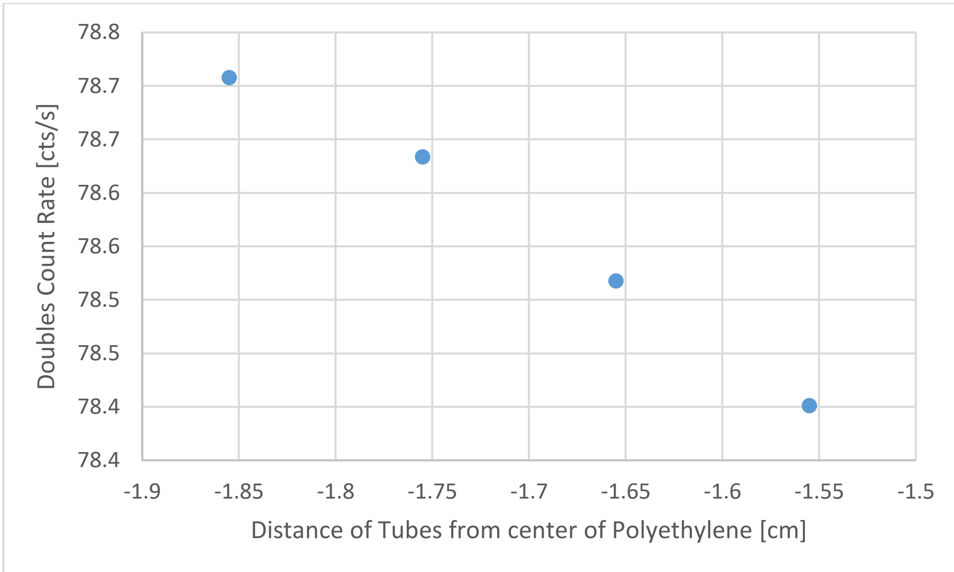

Figure 11: Plot of Doubles count rate (cts/s) vs. the distance of the two tubes to the sides of the central tubes on the long sides of the detector from the center of the polyethylene slabs (cm) for a LWR fuel assembly with a linear density of 60.44 g ^{235}U/cm.

g. Final Design

The final design, based on the results presented above is presented in this section. The final design consists of 28 ^{3}He-tubes at 6 atm pressure. The full design specifications are shown in Figure 12 toFigure 15.

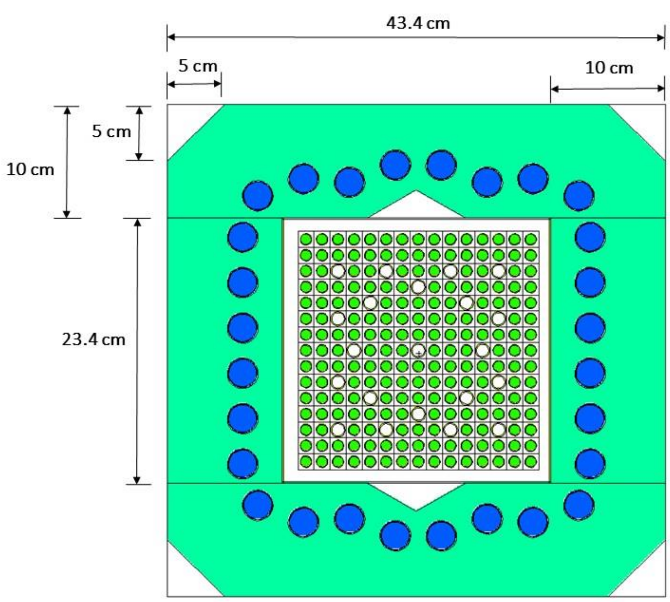

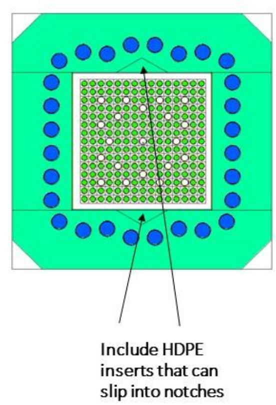

Figure 12: Horizontal dimensions of ^{3}He-based collar.

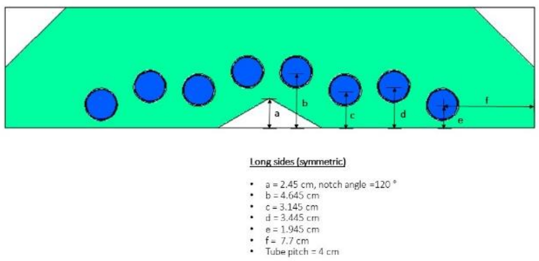

Figure 13: Dimensions of long panels of ^{3}He-based collar.

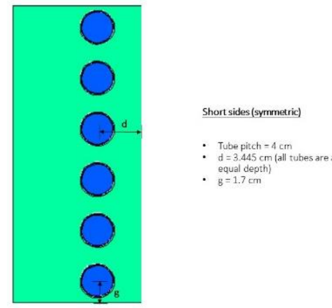

Figure 14: Dimensions of short panels of ^{3}He-based collar.

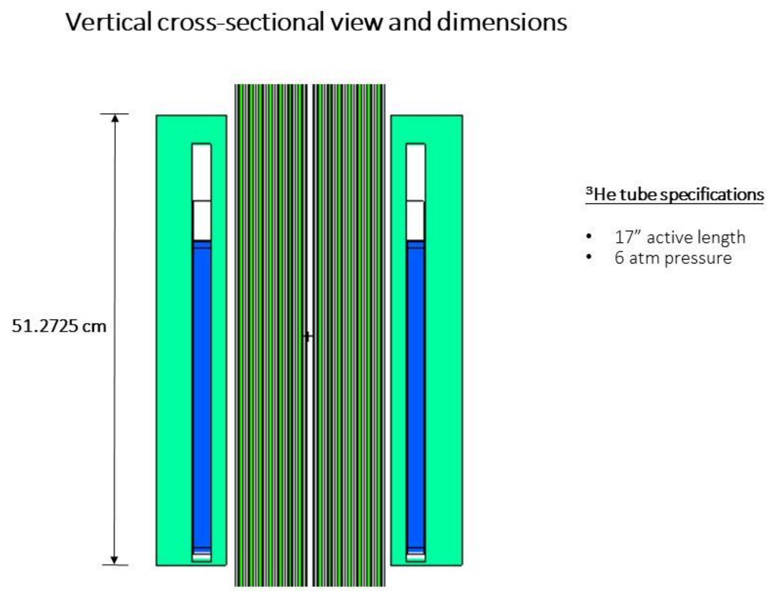

Figure 15: Vertical dimensions of ^{3}He-based collar.

3. ^{10}B-based FNPC Design

The starting point for the optimization of the Boron 10 plate Fast Neutron Passive Collar (FNPC-B10) was based on the final optimized design of an active boron plate collar as designed as part of the FY2016 Rodeo [4]. The parameters for the final optimized design are given in Table 1 and reference [5].

Table 2: Final optimized design parameters for the active boron plate UNCL design from the FY2016 Rodeo I.

Final Boron Plate UNCL Design Characteristics	
Characteristic	Value
Predelay	4.5 μs
Gate Width	64 μs
Front Polyethylene Thickness	0.75 cm
Back Polyethylene Thickness	1 cm
Polyethylene Thickness between cells	0.8 cm
Number of Cells	7
Cd Thickness	0.5 mm
AmLi distance from front face of polyethylene	6.0 cm
Overall Dimensions (width, depth, height)	50.4 cm x 55.8 cm x 51 cm

The starting point for the passive collar design was simply to replace the polyethylene AmLi source holder side with additional boron plate slabs detectors. The Monte Carlo model is shown in Figure 16. The overall height of the boron slab detectors was fixed to 21.5 inches. The thicknesses of the slabs change depending on the polyethylene thickness and number of cells. There are several parameters that were adjusted during the optimization process. These include the number of cells in each slab detector, thickness of the front and back polyethylene layers, and the thickness of the polyethylene layer between the cells.

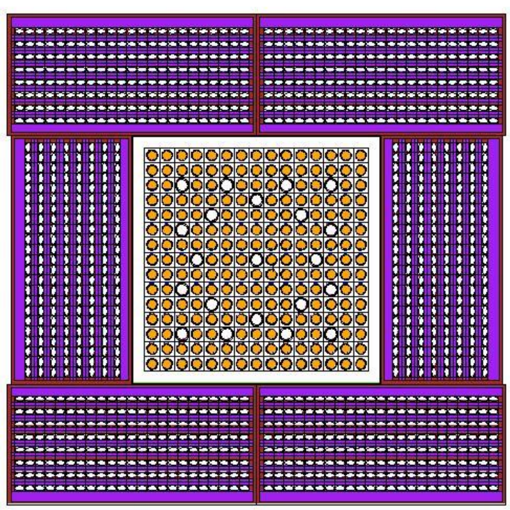

Figure 16: Monte Carlo model of the boron slab based passive neutron collar detector.

For each design, 7 fuel assemblies were modeled with MCNP. These were based on the calibration and poison fuel assemblies used in the FY2016 Rodeo as described in Section 2.

a. Fuel Assembly length

Before beginning the design optimization, a study was conducted to determine the length of fuel assembly that contributes to the detector response. Typical fuel assemblies are on the order of 3 meters long. Two sets of modeling were completed as shown in Figure 17 andFigure 18. One model had a fixed 300 cm long element with source neutrons started in a smaller length centered in the middle of the assembly, which also corresponds to the middle of the detector. These results are shown by the blue points in Figure 17 andFigure 18. The second case modeled the fuel assemblies of various lengths from ± 50 cm to ± 150 cm, with the source particles starting along the entire length of the fuel assembly. This is shown by the red points in Figure 17 and Figure 18. The singles and doubles rates tend to plateau for modeled fuel assemblies greater than 200 cm in length. The difference in response between the two models indicates the contribution to the detector response from induced fission from the nuclear material beyond the source distribution length. Based on the results on this study, all subsequent MCNP modeling was done for a fuel assembly length of 200 cm (or in MNCP space from -100 cm to +100 cm).

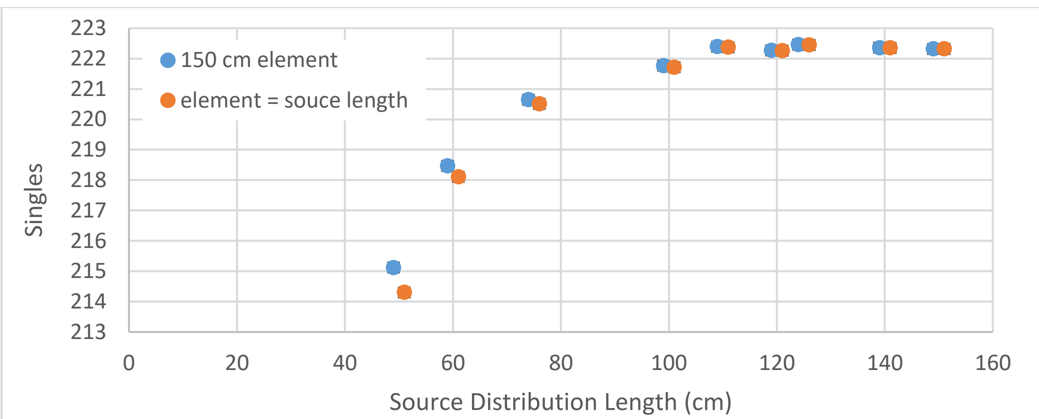

Figure 17: Plot of the Singles rate for various source length starting distributions. Note that the source distribution length and the fuel assembly length are from +/- the length dimension. The source distribution length was slightly offset between the two data sets for easier viewing. The blue dots represent a fixed 300 cm fuel assemblies with source distribution starting lengths varying from +/-50 cm to +/- 150 cm from the center on the middle of the fuel assembly. The red dot represent cases where a shorter fuel assembly was modelled with neutrons starting along the entire length.

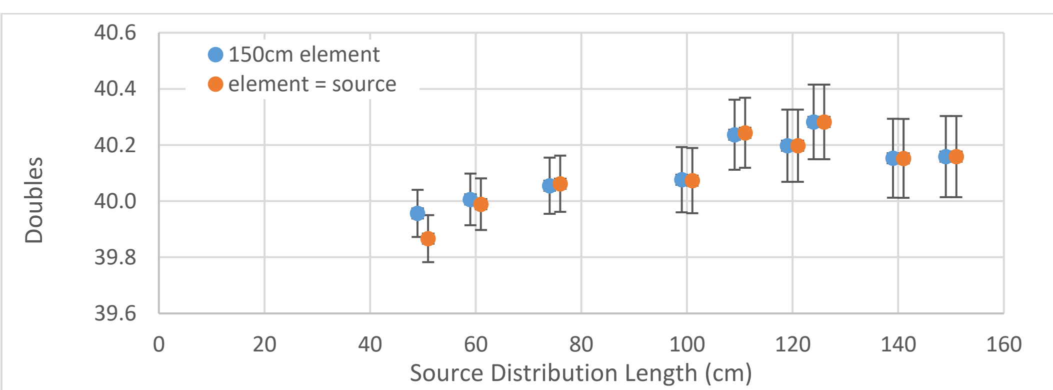

Figure 18: Plot of the Doubles rate for various source length starting distributions. Note that the source distribution length and the fuel assembly length are from +/- the length dimension. The blue dots represent a fixed 300 cm fuel assemblies with source distribution starting lengths varying from +/-50 cm to +/- 150 cm from the center on the middle of the fuel assembly. The red dot represent cases where a shorter fuel assembly was modelled with neutrons starting along the entire length.

b. Liner material, Cd and Gd

Operation of the UNCL in fast mode requires neutron capture liners placed around the inside of the collar well. This liner prevents neutrons that have been thermalized within the polyethylene body of the detector from entering the sample region and inducing fission in the fuel assembly. Since the induced fission cross section is very large at thermal energies, the poison liner will greatly reduce the response of the detector. The advantage of using a poison liner is to make the detector response less sensitive to burnable poisons that are in some fuel assemblies. One of the design goals is to optimize the detector system to be least sensitive to burnable poisons.

A MCNP study was taken to determine the best liner material and thickness to minimize the effect of burnable poison on the detector response. Cadmium and Gadolinium liners of thicknesses 0.5 mm and 1.0 mm were modeled with the standard set of fuel assemblies described above and these results are shown in Figure 19. The 4 LEU calibration fuel assemblies were used to calibrate the doubles rate to the fuel loading in the assembly. For the 3 poison rods, the modeled doubles rate was compared to the calibration doubles rate and this percent difference is shown in Figure 20. The sensitivity to the burnable poison rods was minimized with the 1.0 mm Gadolinium liner. For the case of the 1.0 mm Gd liner, the doubles response and slope of the calibration curve were slightly reduced. These are parameters that we would like to maximize for best optimization. Since the most important factor is to minimize the sensitivity to burnable poison, all subsequent optimization modeling used a 1.0 mm Gadolinium liner

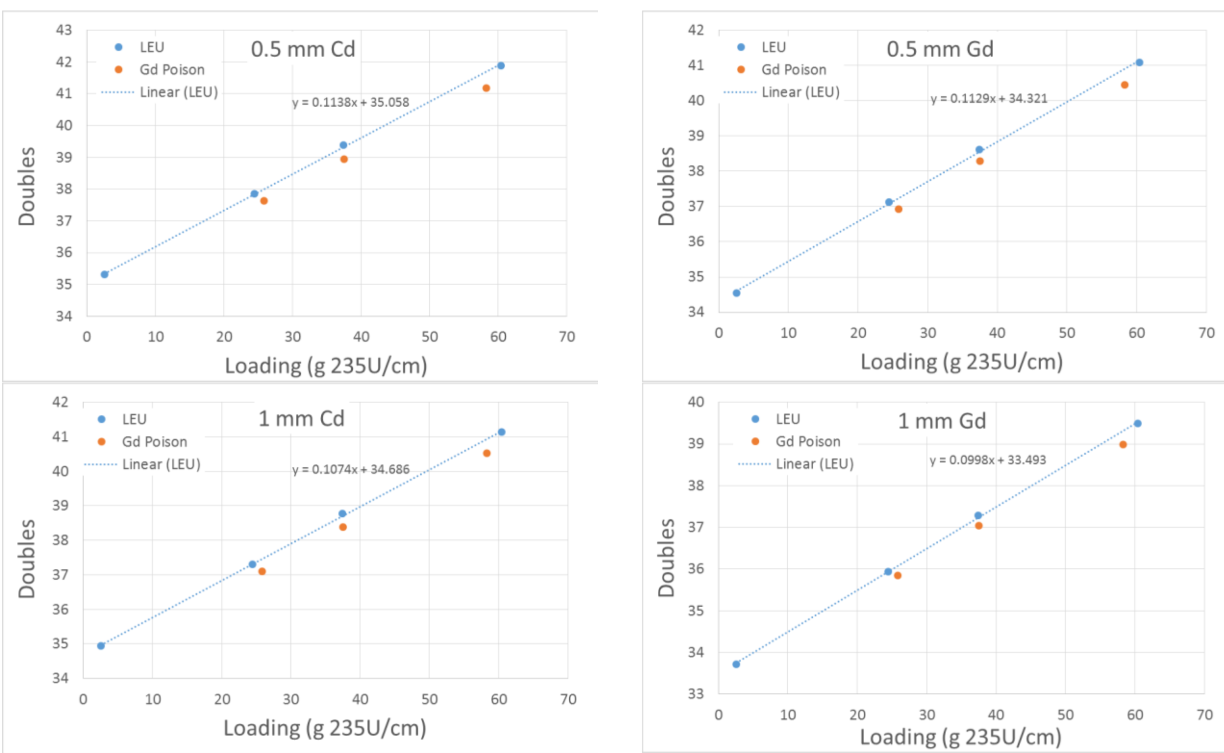

Figure 19: Plots of the doubles versus uranium loading for 4 different liner material configurations. The blue data points are the LEU fuel assemblies and the solid line is the empirical calibration fit to the data. The three red data points are the fuel assemblies containing burnable poison.

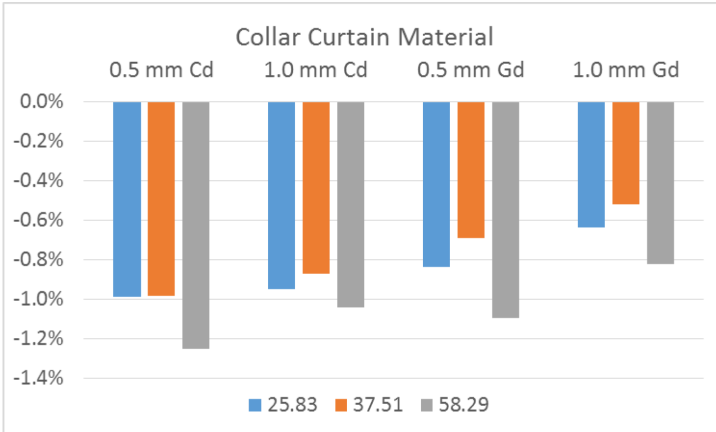

Figure 20: The bias (percent difference between model response and calculated response based on the LEU calibration curve) for the three fuel assemblies containing burnable poison.

c. Number of cells

The first parameter that needed to be fixed was the number of cells to incorporate into each boron slab. The numbers of cells and the practical use of the instrument are in conflict. Increasing the number of cells will results in an increase response. From a usability perspective, the instrument should be made as small and portable as possible. The limiting constraint was to design an instrument that has a similar or smaller footprint than the ^{3}He based UNCL currently in use by the IAEA.

Designs with 6, 7, and 8 cells were modeled. An instrument with more than 8 cells was getting beyond the size and weight constraints for practical use by an inspector in a facility. A comparison of the count rates was made with a 0.75 cm thick front layer of polyethylene, 1.6 cm thick layer of polyethylene between the cells, and 1.0 cm thick back layer of polyethylene. The doubles rate and slope of the calibration curve are shown in Figure 21.

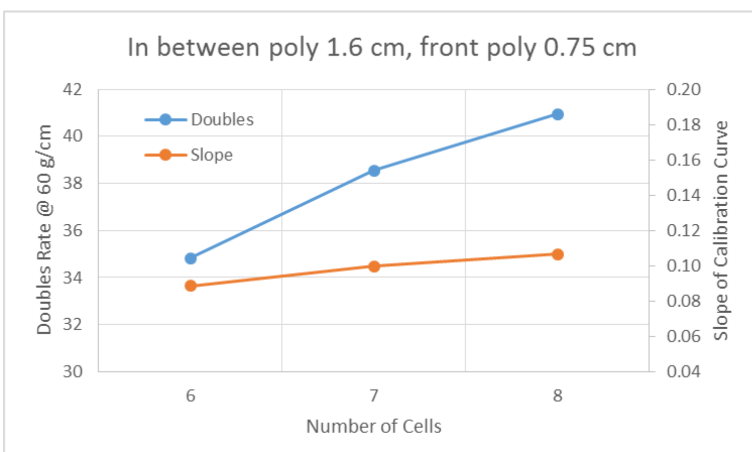

Figure 21: Comparison of the doubles rate and slope of the calibration curve for designs with 6, 7, and 8 cells.

The 8 cell design had the best performance. The increase in performance over the 6 and 7 cell designs are deemed significant enough to justify the additional cost and operational implications. All additional optimization was only performed with 8 cell slabs. The additional refinement in the design included optimizing the polyethylene thickness between cells and the front and back polyethylene thickness.

d. Polyethylene Thickness between cells

The polyethylene thickness between cells was first optimized. The front poly thickness was fixed at 0.75 cm and the back poly thickness was fixed at 1.0 cm. The response of the doubles rate for LEU with 60 g/cm loading and the slope of the calibration curve as the polyethylene thickness between cells was varied from 0.6 cm to 1.8 cm is shown in Figure 22. The best detector response would maximize the doubles rate and the slope of the calibration. The MCNP results show that the double rate maximized at around 1.2 cm of polyethylene thickness and the slope around 1.4 cm of thickness. Since there are 8 cells in this design there are 7 layers of polyethylene between the cells and as a result the overall size of the detector is very dependent on the final polyethylene thickness between cells. To constrain the overall size of the detector, polyethylene thicknesses between cells of 1.0 and 1.2 were chosen for the optimization of the other design parameters.

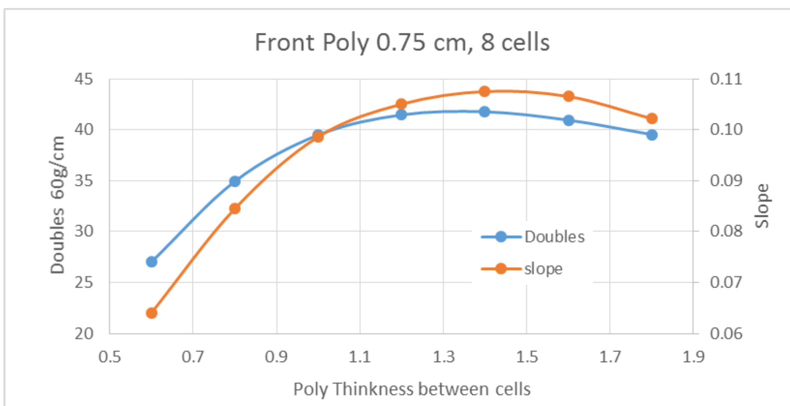

Figure 22: Plot of the double rate and slope of the calibration curve versus the polyethylene thickness between cells. The doubles rate was for the LEU fuel assembly with a ^{235}U loading of 60 g/cm.

e. Front Polyethylene thickness

The optimization of front polyethylene thickness was modeled with 1.0 cm and 1.2 cm thick polyethylene between the cells and 1.0 cm thick polyethylene on the outside. The response of the doubles rate for LEU with 60 g/cm loading and the slope of the calibration curve as the front polyethylene thickness was varied from 0.0 cm to 1.5 cm is shown in Figure 23 andFigure 24. The best optimization occurs with a polyethylene thickness between cells of 1.2 cm and a front polyethylene thickness of 0.5 cm.

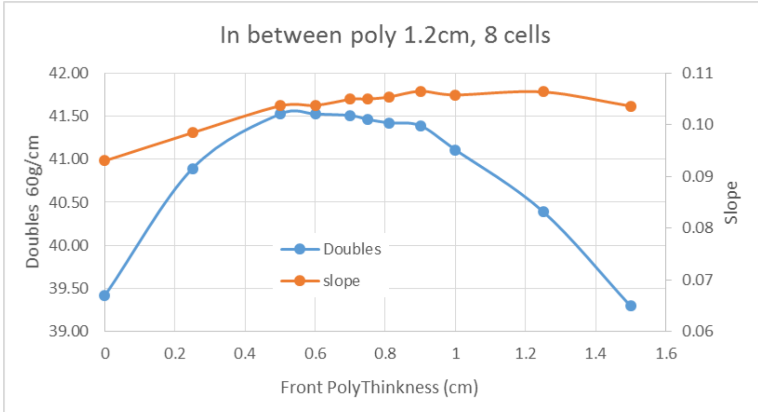

Figure 23: Plot of the double rate and slope of the calibration curve versus the front polyethylene thickness. The doubles rate was for the LEU fuel assembly with a ^{235}U loading of 60 g/cm.

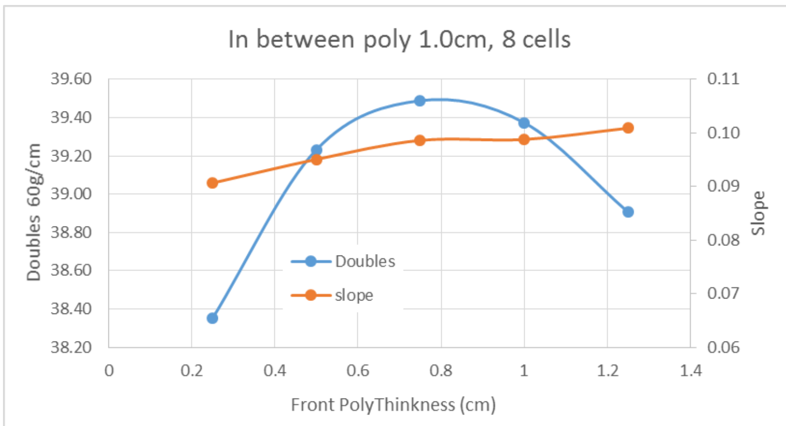

Figure 24: Plot of the double rate and slope of the calibration curve versus the front polyethylene thickness. The doubles rate was for the LEU fuel assembly with a ^{235}U loading of 60 g/cm.

f. Back Poly Thickness

The optimization of back polyethylene thickness was modeled with 1.2 cm thick polyethylene between the cells and 0.5 cm thick polyethylene in front. The response of the doubles rate for LEU with 60 g/cm loading and the slope of the calibration curve as the back polyethylene thickness was varied from 0.25 cm to 1.5 cm is shown in Figure 25. The back polyethylene thickness was chosen to be 1.0 cm.

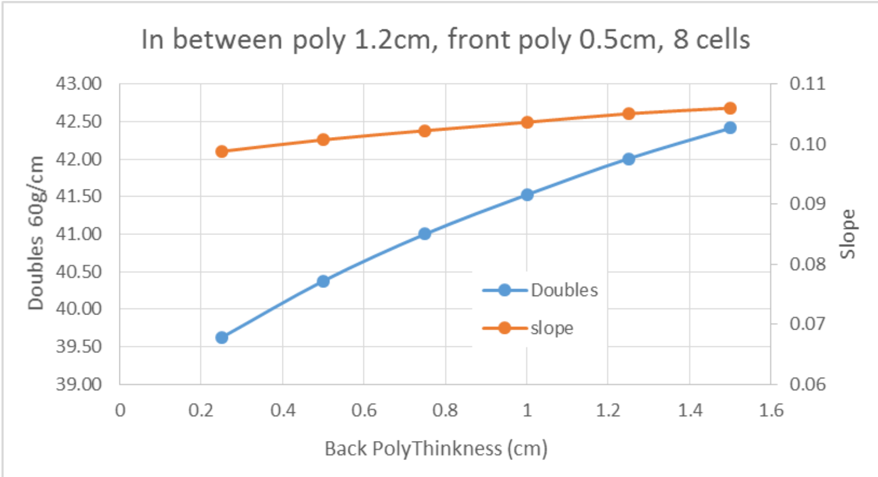

Figure 25: Plot of the double rate and slope of the calibration curve versus the back polyethylene thickness. The doubles rate was for the LEU fuel assembly with a ^{235}U loading of 60 g/cm.

g. Optimized Design

The final optimized design parameters for the boron plate based UNCL as determined by the Monte Carlo simulations are given in Table 3. MCNP diagrams are shown in Figure 26 and Figure 27 for the entire system and for one slab.

Table 3: Optimized designed parameters for the boron plate based UNCL determined from the Monte Carlo simulations.

Parameter	Value
Number of cells per slab	8
Thickness of front polyethylene layer	0.5 cm
Thickness of polyethylene between cells	1.2 cm
Thickness of back polyethylene layer	1.0 cm
Cell Thickness	15.34 cm
Cell Active Length	47.32 cm
Slab Dimensions	23.4 cm x 15.34 cm x 54.61 cm
Full Boron UNCL Dimensions	55.08 cm x 46.8 cm x 54.61 cm

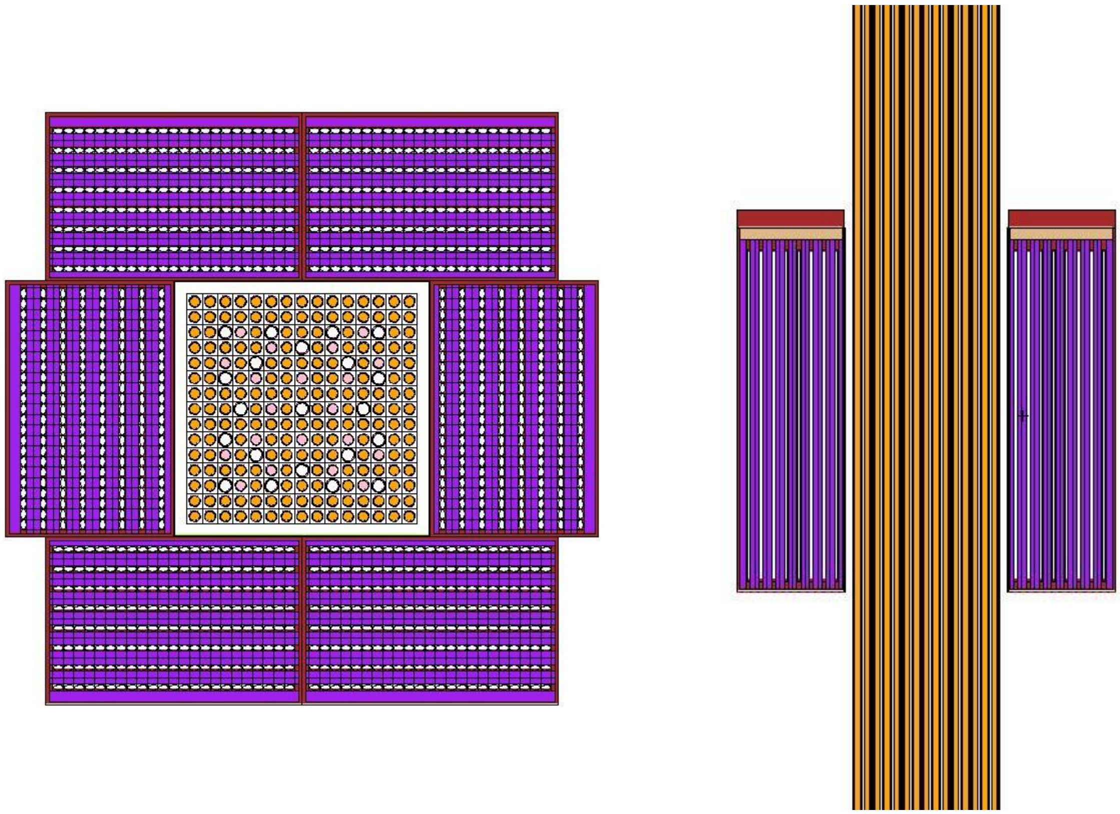

Figure 26: MCNP generated drawings of the optimized boron plate based UNCL system. Shown on the left is a horizontal cut and on the right is a vertical cut. The left drawing consists of 6 boron plate slab detectors arranged into a collar detector surrounding a fuel assembly. In the vertical cut on the right, to slab detectors are seen on either side of the fuel assemble. The top and bottom of the fuel assembly are cutoff in the diagram. The diagrams have different scaling factors.

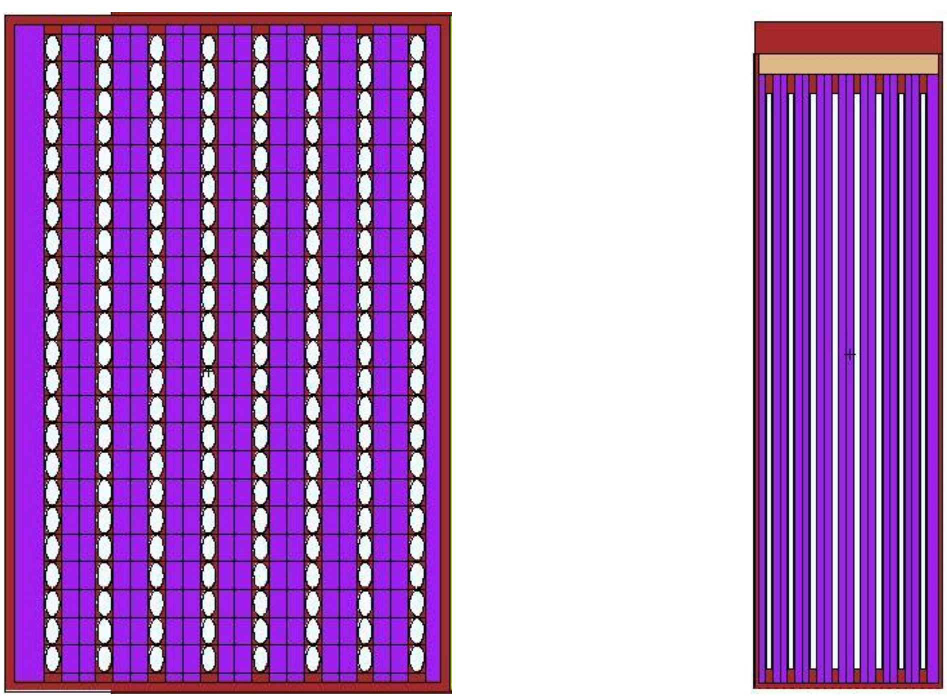

Figure 27: MCNP generated drawings of one boron plate slab detector. Shown on the left is a horizontal cut and on the right is a vertical cut. The left drawing consists of 8 boron plate cells sandwiched between layers of polyethylene. In the vertical cut on the right, the 8 cells can be seen. On the top is the location of the junction box. The diagrams have different scaling factors.

4. Summary

The FNPC is a new, simplified version of the UNCL, which has been optimized using MCNP 6.1 [3] for passive measurements. The FNPC was optimized for two different detection materials, ^{10}B and ^{3}He. The optimization of the two systems considered several factors including the maximizing detector response, minimizing bias caused by burnable poison, minimizing cost, and maximizing usability by IAEA inspectors. The optimized ^{3}He design consists of 4 polyethylene slabs arranged in a square configuration around the fuel assembly. The detector contains 28 ^{3}He tubes with a 43 cm active length at 6 atm pressure. It is optimized to measure both VVER fuel and standard LWR fuel. The optimized ^{10}B slab consists of 6 polyethylene slabs each containing 8 ^{10}B cells in a square configuration around the fuel assembly with active length 47.32 cm.

5. References

[1] Menlove, H. O., et. al. "Neutron Collar Calibration and Evaluation containing Burnable Neutron Absorbers", Los Alamos National Laboratory Report, LA-11965-MS, (1990).

[2] Root, M. A., et al. "Using the Time-Correlated Induced Fission Method to Simultaneously Measure the 235U Content and the Burnable Poison Content in LWR Fuel Assemblies." *Nuclear Technology*, 2018, pp. 1–14.

[3] Werner, C. J., et. al., *MCNP User's Manual v. 6.2*, Los Alamos National Laboratory, LA-UR-17-29981, (2017).

[4] Advanced Neutron Detection Technology Rodeo, A. Belian et al, JRC Conference and Workshop Reports of the ESARDA 39th Annual Meeting, Dusseldort, Germany, 2017, EUR 28795 EN.

[5] W.H. Geist, E. Henzlova, and H.O. Menlove, "Boron Plate UNCL Design" Los Alamos National Laboratory report, LA_UR-16-28617.